BRAIDED ANGLE MEASUREMENT TECHNIQUE FOR THREE-DIMENSIONAL BRAIDED COMPOSITE MATERIAL PREFORM USING MATHEMATICAL MORPHOLOGY AND IMAGE TEXTURE

Wan Zhenkai, Li Jialu

Tianjin Polytechnic University
(Tianjin 300160, People's Republic of China)
E-mail: wanzhenkai@tjpu.edu.cn

Abstract

This paper describes a new measuring algorithm for estimating the exterior average braided angle of a three-dimensional (3-D) braided composite material preform] based on image texture. In this project, an advanced filtered algorithm for an image of a 3-D braided composite material preform is developed on the basis of mathematical morphology. Median filter algorithms for mathematical morphology are applied in the system. The polar spectrum and main properties are investigated in the paper.

Theory shows that a rotated texture's polar spectrum is an approximate translation of the unrotated texture's polar spectrum, and that the degree of each translation approximates to the corresponding rotation of the surface.

The system was tested on both carbon and glass fibre preforms. We have obtained very encouraging experimental results, which show that the proposed method is feasible. So far, the research is a new development for measuring 3-D braided composite material preforms.

The work will lay the foundation for establishing a test standard for 3-D braided composite material in China.

Key words:

mathematical morphology, preform of braided composite material, median filter, texture, braided angle

1. Introduction

The advantages of 3-D braided composite materials are widely known. Composite materials, especially carbon-fibre reinforced plastics, are increasingly often used today in the aerospace, automotive, sports equipment, and other commercial industries because of their advantages over conventional metals. Composites have a high strength-to-weight ratio, and can be constructed to meet specific design needs.

3-D braiding can produce thick and net section preforms, in which tows are so intertwined that there may be no distinct layers. In one process, the yarn carriers are arranged in a two-dimensional grid, often in rectangular or annular patterns, and sometimes in the cross-sectional shape of the final component. Multiple rectangles can be concatenated to form more complex cross-sections. Braiding proceeds by alternately exchanging rows and columns of yarn carriers. While the tracks that move yarn carriers return to their original positions after a small number of steps, the carriers themselves can follow complex paths by passing from one track to another. 3-D braiding can be characterised as 2-step, 4-step, and multistep processes. The number of steps refers to the number of movements required for the yarn carriers to return to their original positions.

The biggest automatic braided machine in China based on 4-step was made by Tianjin Polytechnic University in 1993. It has produced variable preforms of 3-D braided composites material.

In recent years much work has been done on analysing 3-D braided composites material [1,2]. Based on earlier research, much of the work focused on the use of mechanical analysis[3,4]. However the properties of 3-D braided composites material depend most of all on the total volume fraction of all fibres and the proportions of the fibres that point in various directions. It is well known that the total volume fraction has a close relation to integral structures. Various process models have been derived to describe the complex unit cells of 3-D braiding [5]. The relations between the surface yarn angle of inclination and the internal yarn angle of inclination have been researched [6]. It is vitally important to measure the surface preform's braided angle to predict the volume fraction of 3-D braided composite material.

It is important to measure and control the braided parameter for in order to increase the ability of determining the material properties.

However, the surface braided angle of a 3-D braided composite material preform is now done manually, and no method for measuring maturation has yet been established. The tool most frequently used is the protractor; no commercial product for measuring the braided angle exists [7]. The braided angle of 3-D braided material preform is defined as follows: it is the angle formed by braided yarns along the braided direction in the surface. Figure 1 shows the surface graphics of a 3-D braided material preform under ideal condition; Figure 2 shows the practical surface graphics of a 3-D braided material preform. In Figure 1, the parameter θ is a surface braided angle of the 3-D braided material preform. From Figure 2, it is clear that the surface image of the 3-D braided composite material preform yields a two-dimensional (2-D) image.

The evenness of the surface braided angle is closely related to material mechanical performance after the braided perform is reinforced. Using a computer for analysing the surface texture of a 3-D braided material preform is a very important aspect of research [3].

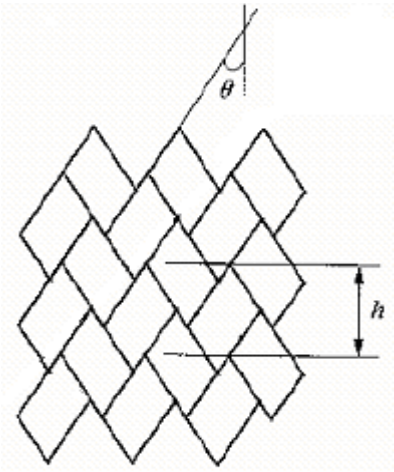

Figure 1. Preform surface graphics

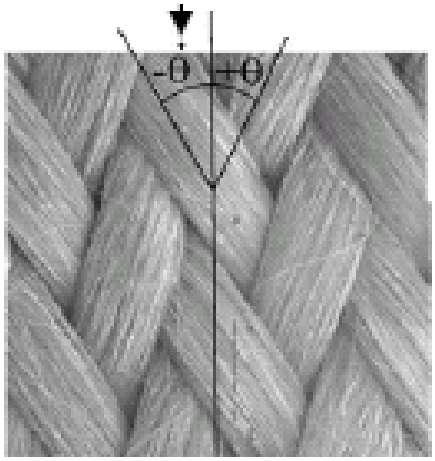

Figure 2. The practical image under ideal preform surface conditions

To solve the above problems associated with algorithms for computing the average surface braided angle, we propose a new non-linear filter technique based on the mathematical morphology. In addition, a texture algorithm based on the Fourier transform can be applied. Experimental results show that the proposed algorithm can be used to measure the preform's average braided angle.

This paper is organised as follows. The system for image acquisition is presented in Section 2, the filter algorithms in Section 3, the measuring method in Section 4. The experimental results are given in Section 5, and finally, concluding remarks and acknowledgements are provided in Sections 6 and 7.

2. The image acquisition system

The surface image testing system diagram for 3-D braided composite material preforms is described as shown in Figure 3. It consists of a CCD camera, an image digitiser card, a computer unit, a monitor and auxiliary equipment.

The digital image technique equipment used to acquire and digitise the video images included a black and white Sony VC-323D camera and a VC512A real-time, grey-level, image digitiser board in a PC. The 512A digitiser card has a 1-Mbyte frame-memory that consists of a dynamic dual RAM (TC524256). The matrix resolution for this particular board was 512 by 512 pixels. The lens used with the video camera was made by Nikon. A high-resolution SON'PVM-14N6E&PVM-14N5E video monitor was used to display the digital image. The illumination source was a 30W electric bulb. The PC and image digitiser board system was used to digitise the video images, which were redisplayed on the video monitor.

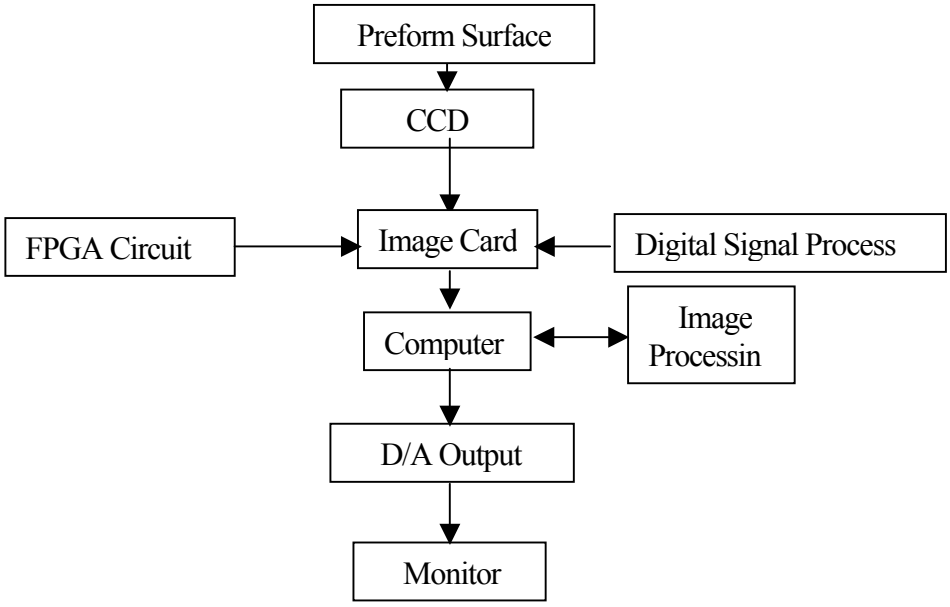

Figure 3. The diagram of 3-D braided preform image process system

The surface image of the preform is covered by an area CCD camera in this system. The digitiser board receives the CCD camera video signal. The digitiser board collects the image within a frequency range of 10to 30 MHz. This is different from other commercial products, as it relies on the digital signal processor and does not require PC to work when collecting and filtering the image signal. The CCD video camera records the surface light intensity pattern as varying levels of grey. To digitise the video signal that represented the light pattern, the video image was divided into an array of equal-area, rectangular pixels. The grey level of each pixel was assigned an integer value from 0 to 255 that was proportional to the light intensity received from the surface of the test object. Pure black was assigned the value 0, and the white was assigned 255, with the values between representing different shades of grey. The integers representing the light pattern of the test object were assigned pixel locations based on an X-Y coordinate system that corresponded to the actual location on the test object. The digital value is stored in frame memory of digitiser board. Through software, the digital value in the frame-memory of digitiser board is sent to a D/A converter at the same time. As the D/A converter passes data to the monitor at constant

television speed, the monitor shows the image. The signal processor can control an active image halt at any time, thus 'freezing' it for further inspection. After freezing, we can always show the frozen image, and then the PC will read the data from frame-buffer. The PC calculates the braided angle through software.

In the system, the digitiser card will occupy the address of the host computer 300 H ~ 30 FH. The host computer may deliver data and accomplish various functions by using these port addresses.

3. Mathematical morphology and median filters

The surface image of the 3-D braided composite material preform presents 2-D periodicity [3]. As the difference between the grey colours at the image edgeis small, it is necessary to filter the surface image in order to enhance it. For the preform image, we do not only detect the edge position but also the image edge orientation. Experiments have proved that a 2-D edge median filter based on mathematical morphology had a better effect for the composite material preform image filtered than any other algorithm, such as the Sobel or the Robert algorithms [9] etc., which although they are classic linear algorithms, have an acute function on edges and are vulnerable to noise. For a braided preform image in which there are many complex surface features, the effect of edge detection is not good.

The theory of mathematical morphology consists of image transformations that are based on set-theoretical, geometrical and topological concepts. Mathematical morphology is useful for the analysis of the geometrical structure, the reduction of clutter, and the implementation of image enhancement and segmentation. It is now widely used for image analysis purposes (i.e. edge detection, shape analysis, image coding, smoothing and thinning).

We define a discrete median filter by considering a uniform discrete measure k defined on a finite number of points $\{x_i \mid i = 1, \ldots, N\}$. This means that k is defined by $|\{x_i\}|_k = 1$, which is to say that Dirac masses δ_i exist at each point x_i , $i \in \{1, \ldots, N\}$. We could normalize k, but this is not necessary, the reason for which will become clear. Translates of the points x_i create the discrete neighbourhood that is used to compute the median value of a function u at a point x. We denote the set of subsets of $\{1, \ldots, N\}$ by $P(N)$ and the number of elements in $P \in P(N)$ by card(P). Since card(P) = $|P|_k$, we will suppress the k-notation is favour of the more transparent 'card(P),' but one should remember that the k measure is still there. Here are the definitions of the two discrete median filters[10]:

$$Medu(x) = \sup_{\substack{P\in(N) \\ card(P)\geq N/2}} \inf_{i\in P} u(x-x_i), \quad (1)$$

$$Med^{-}u(x) = \inf_{\substack{P\in(N) \\ card(P)\geq N/2}} \sup_{i\in P} u(x-x_i), \quad (2)$$

When k was continuous, we could replace '$|B|_k \geq ½$' with '"$|B|_k = 1/2$', but this is not directly possible in the discrete case, since $N/2$ is not an integer if N is odd. To fix this, we define the function M by $M(N) = N/2$ if N is even and $M(N) = (N/2) + (1/2)$ if N is odd. Now we have

$$Medu(x) = \sup_{\substack{P\in(N) \\ card(P)=M(N)}} \inf_{i\in P} u(x-x_i) \quad (3)$$

$$Med^{-}u(x) = \inf_{\substack{P\in(N) \\ card(P)=M(N)}} \sup_{i\in P} u(x-x_i) \quad (4)$$

The fact that we can replace 'card(P) ≥ $N/2$' with 'card(P) = $M(N)$' has been argued elsewhere for the continuous

case; for the discrete case, it is a matter of simple combinatorics. Given any x, let $y_i = u(x-x_i)$. After a suitable permutation of the i's, we can order the y_i as follows: $y_1 \leq, \cdots, \leq y_M \leq, \cdots \leq y_N$. Then for N even,

$$\left\{\inf_{i\in P} y_i \middle| card(P) \geq N/2\right\} = \left\{\inf_{i\in P} y_i \middle| card(P) = M\right\} = \{y_1, ..., y_{M+1}\} \quad (5)$$

$$\left\{\sup_{i\in P} y_i \middle| card(P) \geq N/2\right\} = \left\{\sup_{i\in P} y_i \middle| card(P) = M\right\} = \{y_M, ..., y_N\} \quad (6)$$

and $Medu(x) = y_{M+1} \geq y_M = Med^{-}u(x)$ .If N is odd, we have

$$\left\{\inf_{i\in P} y_i \middle| card(P) \geq N/2\right\} = \left\{\inf_{i\in P} y_i \middle| card(P) = M\right\} = \{y_1, ..., y_M\} \quad (7)$$

$$\left\{\sup_{i\in P} y_i \middle| card(P) \geq N/2\right\} = \left\{\sup_{i\in P} y_i \middle| card(P) = M\right\} = \{y_M, ..., y_N\} \quad (8)$$

and $Medu(x) = Med^{-}u(x) = y_M$. This shows that $Medu(x) = Med^{-}u(x)$. if and only if N is odd.

This discussion shows that the definition of the discrete median filter Med corresponds to the usual statistical definition of the median of a set of data: If the given data consists of the numbers $y_1 \leq y_2 \leq \cdots \leq y_N$ and $N = 2n + 1$, them by definition, the median is y_n+1.In case $N = 2n$, the median is $(y_n + y_n+1)/2$.

The discrete median filters can also be defined in terms of a non-uniform measure k that places different weights on the points x_i. To see what this does, let us assume that the weights are integers k_i, so $|\{x_i\}|_k = k_i$. Then k has total mass $\sum_{i=1}^{n} k_i = K$, and the condition card(P) ≥ N/2 is replaced with $|P|_k \geq K/2$. As before, let $y_i = u(x- x_i)$ and display the data set as $y_1 \leq y_2 \leq \cdots \leq y_N$. Then $Med_k u(x) = y_j$, where j is the largest index such that $k_j + \cdots + k_N \geq N/2$. To see this, let us transform the original ordered sequence into the expanded ordered sequence

$$\underbrace{y_1 = ...y_1}_{k_1} \leq ..... \leq \underbrace{y_i = ...y_i}_{k_i} \leq y_N = ...y_N \quad (9)$$

Then by the definition of j , $y_j \in \{\inf_{i\in P} y_i \mid |P|_k \geq K/2\}$, but yi for $i > j$ is not in this set. Thus, $Med_k u(x) = y_j$ .Conversely, if $Med_k u(x) = y_j$, then y_j is the largest member of the set $\{\inf_{i\in P} y_i \mid |P|_k \geq K/2\}$. This implies that $k_j + \cdots + k_N \geq N/2$, but that $k_i + \cdots + k_N < K/2$ for $i > j$.

If K is odd, what we have just done implies that $Med_k u(x) = Med_k^{-} u(x)$ and that $Med_k u(x)$ is equal to the ordinary median of the ordered set (9).

Finally, we wish to show that the discrete median filter Med is a cyclic operator on discrete images. To be precise, we assume that the digital image u has been periodised so that we have a C-periodic digital image. Assume that the original image defined on the hypercube $[0, 1]^N$ contained n pixels. Then, the total number of grey levels is bounded by n. Since a median filter Med is invariant contrast, the grey levels of Med u are among the original ones. The same is true for the kth iteration Med$^k u$. Since that maximum number of different realisations is n^n, after n^n iterations, there will be two identical images among the images Med$^k u$, $k \in \{1, 2, \ldots, n^n\}$. Thus, Med is cyclic. As a simple example, consider the chessboard image, where $u(i, j) = 255$ if $i + j$ is even and $u(i, j) = 0$ otherwise. When we apply the median filter that takes the median of the four values surrounding a pixel and the

pixel value, it is clear that the filter 'reverses' the chessboard pattern. Indeed, any white pixel (value 255) is surrounded by four black pixels (value zero), so the median filter transforms the white pixel into a black pixel. In the same way, a black pixel is transformed into a white pixel. The effect of a median filter is illustrated in Figure 4.

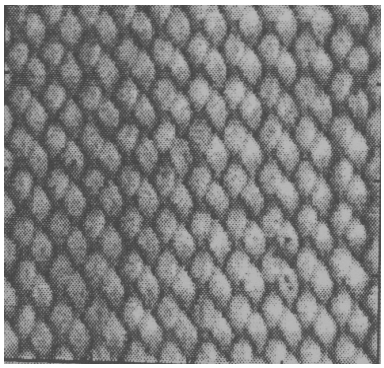

Figure 4a. Original carbon fibre preform surface image

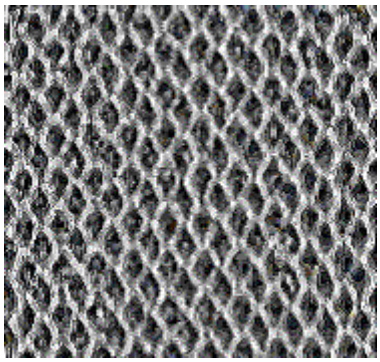

Figure 4b. The result of glass fiber perform surface image using median filter algorithm of mathematical morphology

4. The principle of the braided angle measured for a 3-D braided composite material preform using texture

The important image texture properties are involved in their power spectrum. The spectrum can be worked out by use of the Fourier transform. The image power spectrum may describe the directionality of periodic patterns. The algorithm is based on the 2-D Fourier transform.

The polar spectrum can be used to generate the rotation invariant features which are sensitive to texture directionality, and capture the directionality of textures at different orientations [11].

The polar spectrum is calculated by integrating all the contributions (or values) along a line of orientation β passing through the origin in the image of the gradient spectrum $M(\omega,\beta)$. We can then calculate the function of the polar spectrum $\Pi(\beta)$ as folllows:

$$\Pi(\beta)=\int_0^{\infty} M(\omega,\beta)d\omega \quad (11)$$

This means that the polar spectrum adds the magnitudes of all frequencies in one certain direction β to produce a measure for the intensity in this direction. All these frequencies lie in a radial line. The output of the polar spectrum is the variance as a function of the angle β .This plot is used for illustrating directionality in the image.

Two of the main properties of the polar spectrum were investigated:

(1) the polar spectrum as a function of texture directionality, and
(2) the polar spectrum as a function of surface orientation.

We must note that

$$\Pi_{\phi}(\beta) = \int_{0}^{\infty} M_{\phi}(\omega, \beta) d\omega = \int_{0}^{\infty} M(\omega, \beta + \phi) d\omega = \Pi(\beta + \phi), \quad (12)$$

thus a rotation of ϕ of a surface produces a translation of ϕ in the polar spectrum. The polar spectrum $\Pi(\beta)$ is derived from the gradient spectrum $M(\omega, \beta)$ simply by expressing the spectrum in polar coordinates. It is obvious that the texture's gradient spectrum are rotation-dependent, and that it is a periodic function of β with a period of π.

This shows that a rotated texture's polar spectrum is an approximate translation of the unrotated texture's polar spectrum, and that the degree of each translation approximates to the corresponding rotation of the surface.

The polar spectrum is calculated by using a discrete FFT. Hence the polar spectrum $\Pi(\beta)$ is obtained by summing discrete coefficient values:

$$\Pi(\beta) = \sum_{\omega=1}^{R} M(\omega, \beta) \quad (13)$$

where *R* is the radius high frequency range of a circle centre at the origin. For an $N \times N$ gradient spectra $M(\omega, \beta)$, *R* is typically chosen as *N*/2. The process of the extraction is illustrated in Figure 5.

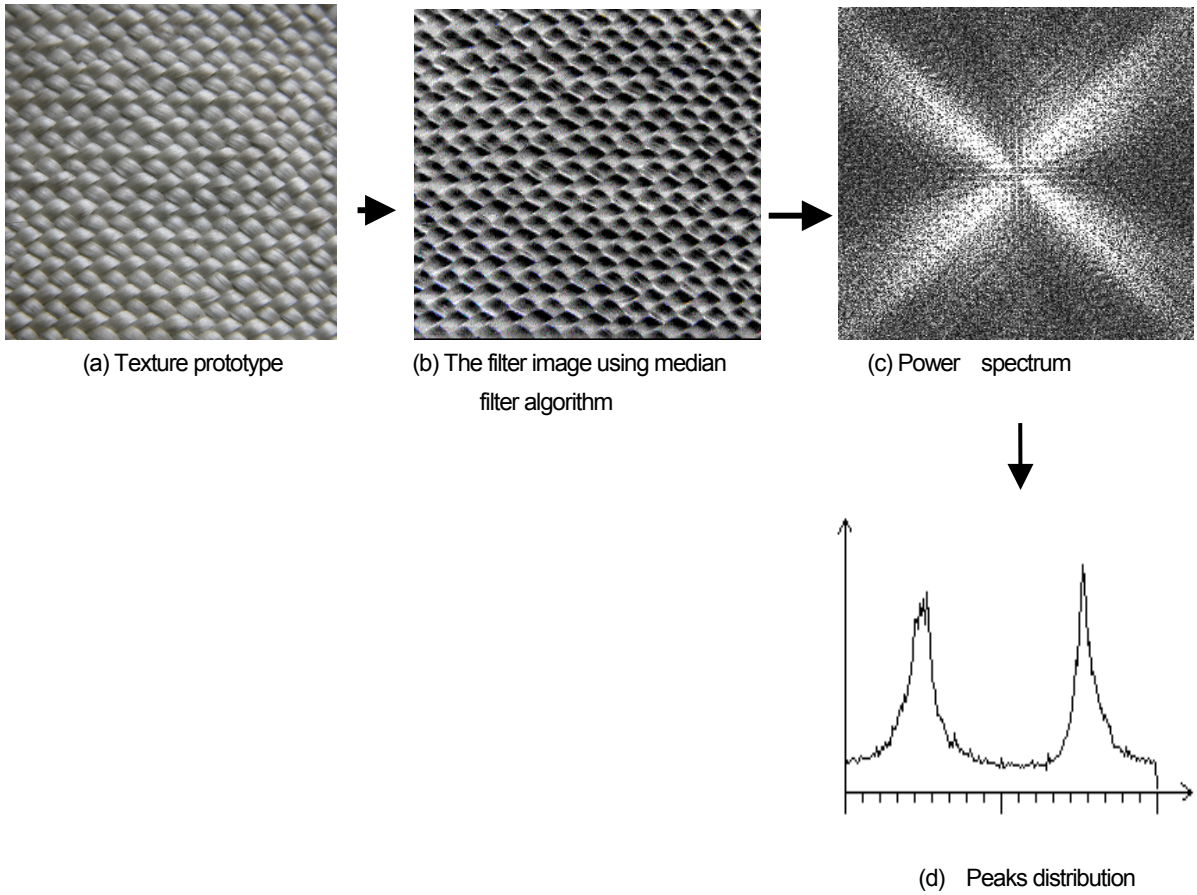

(a) Texture prototype (b) The filter image using median filter algorithm (c) Power spectrum

(d) Peaks distribution

Figure 5. The schematic diagram of polar spectrum extraction

In the image polar spectrum, the prominent peak presents the principal direction of the texture pattern, and the location of peak presents the fundamental spatial period of the pattern.
From Figure 5, we may measure the direction of the original image by using two of the peaks [13]. If the positions of the two peaks are ω_1 and ω_2 at X axis, the average braided angle is described as follow:

$$\bar{\partial} = \frac{\left|(\omega_1+90)-(\omega_2-90)\right|}{2} \quad (14)$$

This is a new algorithm for measuring the braided angle.
In this work, the VC++ language is used. The operation process is shown in Figure 6.

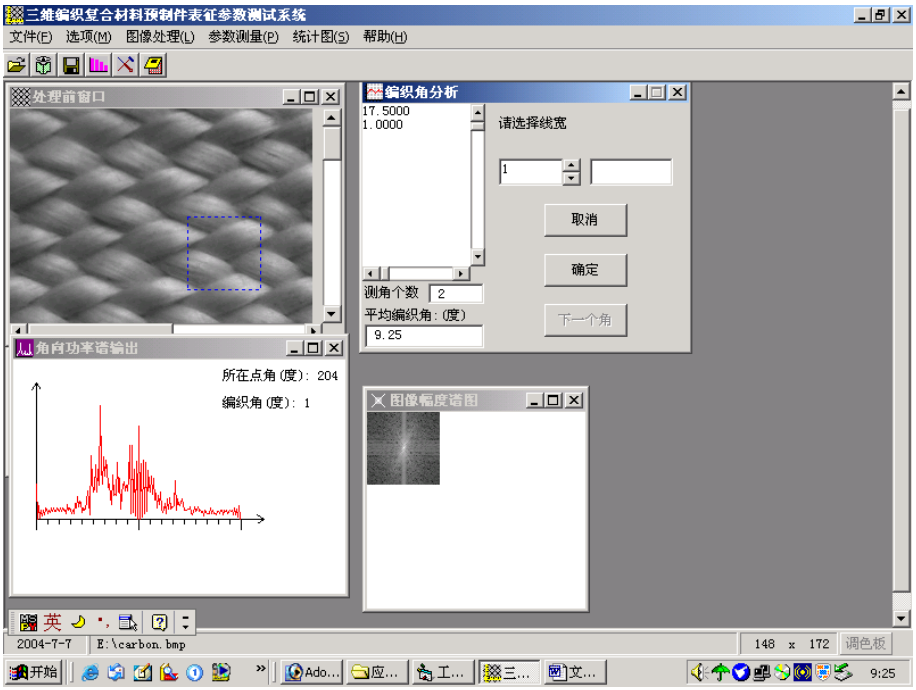

Figure 6a. The screenshot of braided angle tested for glass fibre preform

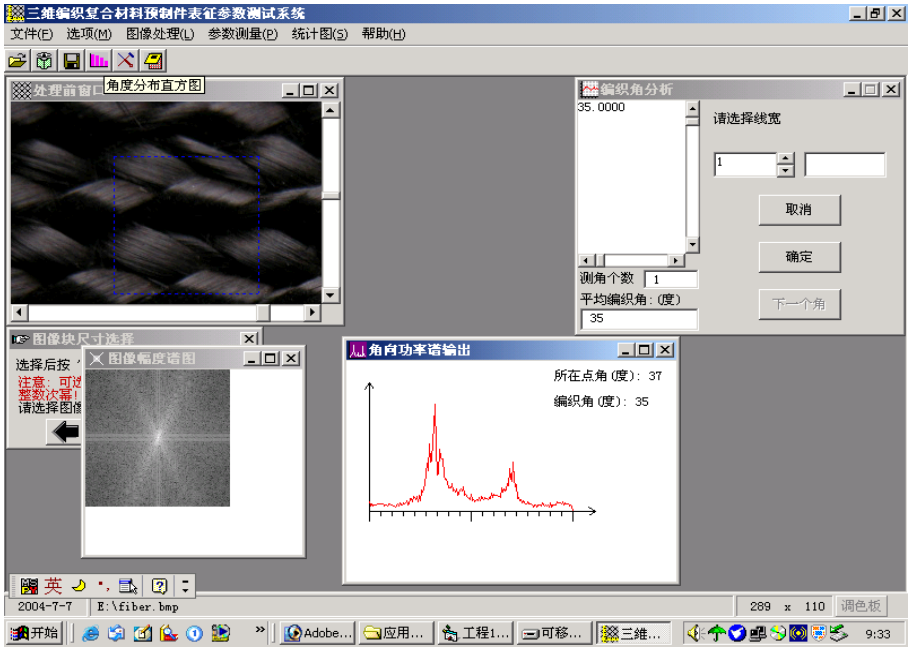

Figure 6b. The screenshot of braided angle tested for carbon fibre perform

5. Experimental results

In order to verify the reliability of the system, we measured a standard image using the above deduction. Figure 7(a) is a original standard image, and Figure 7(b) is the texture diagram of the standard image. Figure 7(c) is the polar power spectrum of a standard image. There are two peaks in Figure 7(c), and each peak presents its texture properties. We may make out the angle formed by the image texture through the distance between the two peaks. Through operating the software, we establish that the standard image angle is 90.1 degrees, which proves that this algorithm is correct.

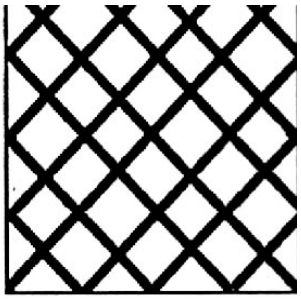

Figure 7a. Standard image

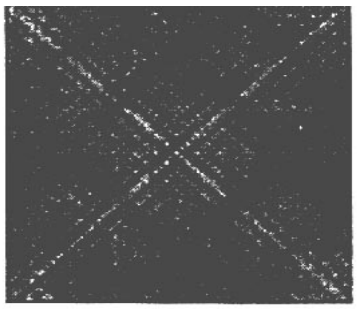

Figure 7b. Texture diagram of standard mage

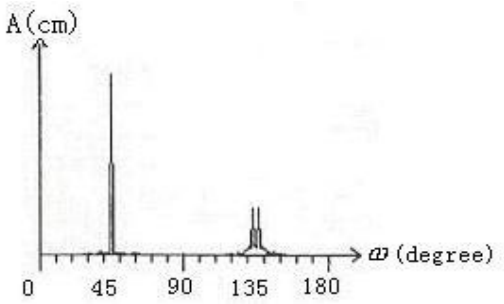

Figure 7c. Polar power of standard image

Figure 8 is the experimental about 3-D braided composite material preform made up carbon fibre. Figure 8(b) shows one peak at 35 degrees and another at 145.5 degrees. The surface braided angle is 39.8 degrees as measured by hand, and 39.1 degrees as measured by the system.

Figure 8a. Original surface

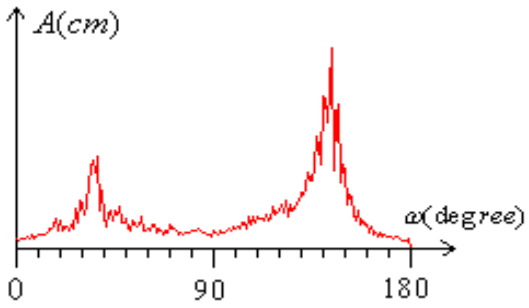

Figure8b. Polar power diagram of carbon fibre preform image

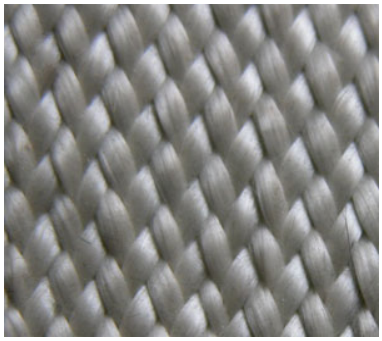

Figure 9a. Original surface

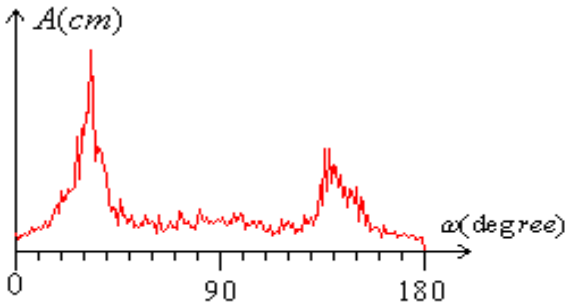

Figure9b. Polar power diagram of fibre glass preform image

Figure 9 shows the experimental results of the 3-D braided composite material preform that made up the glass fibre. Figure 9(b) shows one peak at 32.3 degrees and another at 139.7 degrees. The surface braided angle is 36.3 degrees as measured by hand with a protractor, and 36.1 degrees as measured by this algorithm.

6. Concluding remarks

In this project, we have applied spectrum analysis to 3-D braided composite material preform surface images. The method discussed has proved to be reasonable for measuring the surface braided angle of 3-D composite materials. It will lay the foundation for computer parameter testing to be applied in braided texture analysis.

Braided angle is related to the mechanical performance of composites. In this paper, we discussed the measuring algorithm and the method for obtaining the braided angle of a preform surface image. This is groundwork for analysing the mechanics of 3-D composite material. In future work, we will discuss the precise relation between mechanical properties and the unevenness of the braided angle.

Acknowledgment

This work has been supported by the Composite Material Research Institute of Tianjin Polytechnic University.

The work is supported by the Natural Science Foundation of Tianjin (Grant No. 043600711) and supported by the Ministry of Education Foundation of China (Grant No. 03008).

References

1. *T. W. Chou and F. K. Ko, Textile structural composites, Elsevier New York,1989.*
2. *Gowayed,Yasser; Hwang, Jhy-Cherng; Chapman, Daryl, 'Thermal conductivity of textile composites with arbitrary preform structures', J. of Composites Technology & Research, 17 (1995), pp. 56-62.*
3. *Z.K. Wan, J.L.Li, 'A Research on Surface Braiding Angle Parameter Testing and Unevenness Analysing of 3-D Braiding Composite Preform',,J. of Textile Research. 20 (1999), pp. 363-365.*
4. *Degrieck, J and van Paepegem W, 'Fatigue Damage Modelling of Fibre-Reinforced Composite Materials: Review', Applied Mechanics Reviews,54 (2001),pp. 279-300.*
5. *Miravete, A., 3-D textile reinforcements for composite materials, Woodhead Publishing Limited (Spain), 1999.*
6. *Kalidindi S.R. and Abusafieh A., 'Longitudinal and Transverse Moduli and Strengths of Low Angle 3-D Braided Composites', Journal of Composite Materials, 30 (1996), pp. 885-905.*
7. *Chen Li, Li Jialu, 'Yarn Architecture of 3-D Rectangular Braided Preforms', Acta Material Compositae Sinica, 17 (2000), pp. 1-5*
8. *The appraisal report, Science & Technology Committee of Tianjin,China.2003.*
9. *A. K. Jain, Fundamentals of Digital Image Processing, Prentice-Hall Inc., Englewood Cliffs, New Jersey, 1989.*
10. *http://www.cmla.ens-cachan.fr/Utilisateurs/morel/gmChap09.pdf*
11. *http://www.cee.hw.ac.uk/texturelab/publications/phds/jerryWu/HTML_FinalVersion/chapter6.htm*

∇Δ